Maintaining Robust Stability and Performance through Sampling and Quantization

Mircea Șușcă, *Member, IEEE*, Vlad Mihaly, *Member, IEEE*, and Petru Dobra, *Member, IEEE*

***Abstract*— The inherent problem with continuous-time robust control synthesis is that it returns a controller which cannot directly be implemented on a numeric device. The discrete-time robust control synthesis does not fully solve this problem, as the sampling rate is considered as an input hyperparameter, without explicitly performing a selection, and the quantization of the controller coefficients is not encompassed in the synthesis procedure. The aim of this paper is to provide rigorous means to efficiently compute the sampling rate and quantization step for a given continuous regulator in order to maintain the robust stability and robust performance specifications guaranteed in the analog domain, assuming a constant rate and fixed-point arithmetic, using the structured singular value framework and global optimization techniques. A numerical example is further presented and discussed, emphasizing practical implications.**

I. Introduction

A. Literature Review

Continuous-time robust control synthesis has been employed in a wide range of practical applications, with great flexibility. It provides a general framework to model the nominal industrial process in transfer matrix form or state-space representations, extend it with several approaches to model uncertainties [1], specify performance indices through open- [2] and closed-loop shaping [3], to synthesize unstructured regulators with the aid of algebraic Riccati equations and linear matrix inequalities [4], or to consider fixed-structure controller forms computed through nonsmooth optimization techniques [5], [6]. The $\mathcal{H}_2$ and $\mathcal{H}_\infty$ norms are commonly-used to quantify the performance of a system, for continuous and discrete cases alike, such as in [7] and [8]. The approach of using the $\mathcal{H}_2/\mathcal{H}_\infty$ norms was further extended by the structured singular value (SSV) μ which adequately accounts for uncertainty in the plant dynamics [5], [9]. This framework allows an intuitive application of the main loop theorem [4] in order to guarantee robust stability (RS) and robust performance (RP) of the closed-loop system [3]. Robustness analysis methods in presence of parametric and switching uncertainties have also been introduced in [10].

On the other hand, to implement continuous regulators on a numeric device, two additional procedures must be applied: a sampling operation, leading to a discrete-time model, along with a quantization operation, which applies to both the regulator signals and its coefficients, while the latter problem is maintained even with discrete-time regulator designs.

The sampling period leads to the compromise of selecting a low value which leads to better fidelity [11], [12], with the cost of high microprocessor loads in order to be successfully implemented, and a higher value which becomes desirable with respect to implementation aspects, buy may lead to unsatisfactory performance degradation [13], [14]. The sampling rate yields strong limitations on the μ-synthesis procedure due to arising numerical issues, as specified in [15]. With the recommendation that the sampling times must be selected such that the significant dynamics of the system and weighting functions should not be more than a decade or two below the theoretical Nyquist frequency, the proposed alternative is to design the regulator in continuous-time. This approach would prove to be feasible given that an adequate method to ascertain the quality of the discretized regulator is also available, which is one of the scopes of the current paper.

The quantization effects bring nonlinear behaviour which perturbs the asymptotic stability of the closed-loop system with the appearance of limit cycles in the steady-state response [16], alongside degradations of the transient response, as presented in [17], and reachability limitations [18].

B. Motivation and Contributions

The motivation of this paper is given by the following problems related to discretization and quantization, starting from a satisfactory continuous-time designed controller, i.e. which fulfills RS and RP: (i) the selection of the sampling rate and discretization method may lead to stability losses for initially stable open-loop process models, in addition to destabilizing the closed-loop control system through an inadequate numeric regulator; (ii) discretization may lead to the loss of controllability for the process model [19], [20], which is an inherent problem in the case of Hardware-in-the-Loop simulators, where testing a control law on hardware mimicking the real process can lead to discrepancies between the properties of the continuous-time system and its discrete-time counterpart; (iii) quantization effects are usually studied for the nominal model, not on the entire uncertainty family; (iv) in low-power embedded applications, fixed sampling and quantization rates are desirable, due to their simplicity and while also being ubiquitous in many industrial applications.

The main contributions of the paper are to: (a) provide a joint optimization approach for the sampling rate and quantization step while ensuring RS and RP through the structured singular value framework; (b) present an approach

This paper was financially supported by the Project "Entrepreneurial competences and excellence research in doctoral and postdoctoral programs - ANTREDOC", project co-funded by the European Social Fund financing agreement no. 56437/24.07.2019.

All authors are with Department of Automation, Technical University of Cluj-Napoca, Romania (emails: mircea.susca@aut.utcluj.ro, vlad.mihaly @aut.utcluj.ro, petru.dobra@aut.utcluj.ro).

to reuse the mathematical models of the augmented plant developed in the continuous domain to the discrete domain also, without affecting its conservativeness; (c) describe an approach to assert the quality of a sampling rate and quantization step pair through the sensitivity analysis of its vicinity in the searching space using the condition number.

C. Paper Structure and Notations

The remainder of the paper is structured as follows: Section II provides a short background on robust control techniques; Section III describes the mathematical formulation of the two nonlinear programming problems with robustness constraints, with auxiliary modelling and numerical analysis results; Section IV presents a numerical case study, suggesting an end-to-end approach from the design of a continuous robust controller up to the selection of numerically sound sampling and quantization rates while maintaining robust stability and performance, closing with concluding remarks and future research directions in Section V.

Notations: The two-dimensional optimization variable used throughout the paper will be denoted $\xi = (\tau, q) \in \mathbb{R}^2_+$. Continuous-time systems will be defined on the space $\mathcal{G}$ and denoted with capital italic letters as conventionally used in literature: G, P, K, while their discretized (and also with quantized coefficients with regards to regulator models) counterparts will be defined in the space $\mathcal{G}_D$ and denoted by $\widetilde{G}, \widetilde{P}, \widetilde{K}$ etc. In the same manner, regarding their frequency responses, for the continuous-time case, the transfer matrices will be implicitly evaluated at $j\omega$, i.e. $\{G, P, K\}\big|_{j\omega}$, while their discrete counterparts will be evaluated at $e^{j\omega\tau}$: $\left\{\widetilde{G}, \widetilde{P}, \widetilde{K}\right\}\Big|_{e^{j\omega\tau}}$.

II. Robust Control Background

A generalized continuous-time state-space plant model as used in the robust control framework, Figure 1–a), is defined:

$$P: \begin{pmatrix} \dot{\mathbf{x}}(t) \\ \mathbf{v}(t) \\ \mathbf{z}(t) \\ \mathbf{y}(t) \end{pmatrix} = \left(\begin{array}{c|ccc} A & B_d & B_w & B_u \\ \hline C_v & D_{vd} & D_{vw} & D_{vu} \\ C_z & D_{zd} & D_{zw} & D_{zu} \\ C_y & D_{yd} & D_{yw} & D_{yu} \end{array}\right) \begin{pmatrix} \mathbf{x}(t) \\ \mathbf{d}(t) \\ \mathbf{w}(t) \\ \mathbf{u}(t) \end{pmatrix}, \tag{1}$$

having the control input vector $\mathbf{u} \in \mathbb{R}^{n_u}$ and measurement output vector $\mathbf{y} \in \mathbb{R}^{n_y}$. Additionally, it hosts an exogenous input vector $\mathbf{w} \in \mathbb{R}^{n_w}$, a performance output vector $\mathbf{z} \in \mathbb{R}^{n_z}$, a disturbance input vector $\mathbf{d} \in \mathbb{R}^{n_d}$ and a disturbance output vector $\mathbf{v} \in \mathbb{R}^{n_v}$. The nominal subsystem used in classical control theory is the plant model $G_n = (A, B_u, C_y, D_{yu})$.

The uncertainties considered for the generalized plant P can be classified in: unstructured, used to describe residual dynamics, and structured, which model inaccurate component characteristics. The uncertainty block has the structure:

$$\mathbf{\Delta} = \{\text{diag}(\Delta_1, \ldots, \Delta_f, \delta_1 I_{n_1}, \ldots, \delta_s I_{n_s})\}, \tag{2}$$

where $\Delta_i \in \mathbb{R}^{m_i \times m_i}$ is used for unstructured uncertainties and $\delta_i I_{n_i}$ is used for structured uncertainties. The generalized plant presents an upper linear fractional transform (ULFT) interconnection with the uncertainty block $\mathbf{\Delta}$ and a lower

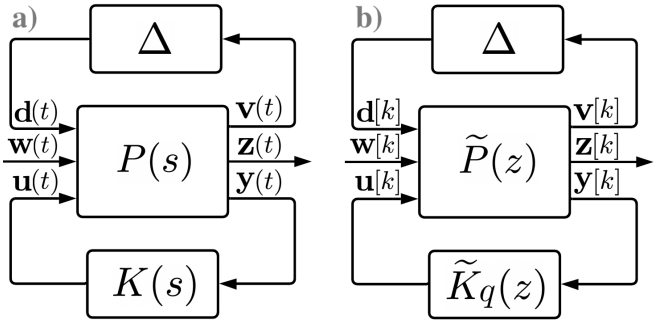

Fig. 1. a) Continuous-time augmented plant P in a ULFT connection with an uncertainty block Δ and LLFT connection with the regulator K; b) Discrete-time equivalents with sampled and discretized blocks, denoted by $\widetilde{P}$, $\widetilde{K}$, and quantized regulator coefficients, further symbolized by $\widetilde{K}_q$.

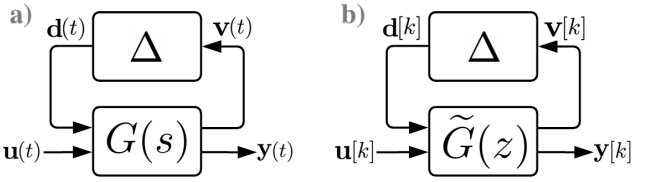

Fig. 2. Uncertain plant model ULFT connection in the continuous-time case a) and discrete-time case b), linking the nominal plant G_n, uncertainty weights U and normalized block Δ as in relation (7).

linear fractional transform (LLFT) interconnection with the controller K, as in Figure 1–a). For the classical robust control problem, the $\mathcal{H}_\infty$ norm is used in the cost functional. On the other hand, in the generalized Robust Control Framework the structured singular value is used. According to the main loop theorem [4], the condition for a controller K to ensure both robust stability (RS) and robust performance (RP) is:

$$\mu_{\mathbf{\Delta}}(\texttt{LLFT}(P, K)) < 1, \tag{3}$$

where $\mu_{\mathbf{\Delta}}(\texttt{LLFT}(P, K))$ is the structured singular value of the LLFT connection between the plant P and controller K according to the uncertainty block $\mathbf{\Delta}$, defined as:

$$\mu_{\mathbf{\Delta}}(\texttt{LLFT}(P, K)) = \sup_{\omega \in \mathbb{R}_+} \frac{1}{\min\limits_{\Delta \in \mathbf{\Delta}} \{\overline{\sigma}(\Delta),\ \det(I - M_\omega \Delta) = 0\}}, \tag{4}$$

where $M_\omega := \texttt{LLFT}(P, K)(j\omega)$. However, the optimization problem is NP-hard and needs to be approximated in order to obtain a polynomial-time counterpart. Such an approximation can be performed using the upper bound from [9]:

$$\mu_{\mathbf{\Delta}}(\texttt{LLFT}(P, K)(j\omega)) \leq \inf_{D \in \boldsymbol{D}} \overline{\sigma}(D \cdot \texttt{LLFT}(P, K)(j\omega) \cdot D^{-1}), \tag{5}$$

having the auxiliary set $\boldsymbol{D}$ defined as:

$$\boldsymbol{D} = \{\text{diag}(d_1 I_{m_1}, \ldots, d_f I_{m_f}, D_1, \ldots, D_s)\}, \tag{6}$$

where $D_i = D_i^\top \in \mathbb{R}^{n_i \times n_i}$.

The regulator K can be synthesized in either an unstructured state-space form, as in [1], or using a fixed-structure form, through nonsmooth optimization approach of [6]. Either approach can be considered for the next section, as long it allows a (possibly sparse) state-space representation.

III. Proposed Method

A. Mathematical Framework

Consider a continuous-time generalized plant model P as in (1), with its nominal process $G_n = (A, B_u, C_y, D_{yu})$ and uncertainty blocks $\Delta \in \mathbf{\Delta}$ having the structure of (2).

The uncertain plant $G_{\mathbf{\Delta}} \equiv G$, Figure 2–a), can be written as a function of the structured normalized uncertainty block $\mathbf{\Delta}$ of corresponding dimension with an adequate mapping:

$$\mathcal{T} : \mathcal{G}^2 \to \mathcal{G},\ G = \mathcal{T}(G_n, U),\ \Delta \in \mathbf{\Delta},\ \|\Delta\|_\infty \leq 1, \quad (7)$$

having the transfer matrix U partitioned as (2). As such, the nominal plant model becomes $G_n = G_{\mathbf{\Delta}}|_{\Delta=O}$. Additionally, the augmented plant P is assumed to be written based on the uncertain plant G through an adequate mapping $\mathcal{A}$ as:

$$\mathcal{A} : \mathcal{G} \times \mathcal{G} \to \mathcal{G},\ P = \mathcal{A}(G, W), \quad (8)$$

with a transfer matrix W hosting the performance filters. As such, G_n has the interface $\mathbf{u} \mapsto \mathbf{y}$, G extends it with $\mathbf{d} \mapsto \mathbf{v}$, while P adds the final components $\mathbf{w} \mapsto \mathbf{z}$ as in (1).

Example 1: To illustrate the above notations, consider an example with a SISO nominal plant $G_n{=}G_{n_1}G_{n_2}$, with multiplicative and additive uncertainties, $U = \begin{bmatrix} U_1 & U_2 \end{bmatrix}$, i.e. $G = G_{n_1}(1{+}U_1\Delta_1)(G_{n_2}{+}U_2\Delta_2)$, $\Delta = \text{diag}\left(\begin{bmatrix}\Delta_1 & \Delta_2\end{bmatrix}\right)$, $\|\Delta\|_\infty \leq 1$, and its augmented plant model using the closed-loop sensitivity weight $W{=}W_S$ as $P = \begin{bmatrix} -W_S G & W_S \end{bmatrix}$. □

Consider that the pair (A, B_u) is stabilizable and the pair (C_y, A) is detectable, assumptions necessary for the existence of a stabilizing controller K [4]. As such, consider a stabilizing regulator $K = (A_K, B_K, C_K, D_K)$ with signal dimensions (n_y, n_K, n_u), which further manages to fulfill the RS and RP specifications for P considering the uncertainty dynamics U, blocks $\Delta{\in}\mathbf{\Delta}$ and specifications W.

The numeric regulator $\widetilde{K}$ is obtained through sampling with a fixed period $\tau \in \mathbb{R}_+$, followed by a discretization of K and, finally, by a quantization of its coefficients with a fixed step $q \in \mathbb{R}_+$. Denoting $\xi = (\tau, q) \in \mathbb{R}_+^2$, we have:

$$\widetilde{K}_q = \mathcal{Q}\{\mathcal{D}\{K, \tau\}, q\} = \mathcal{Q}\left\{\widetilde{K}, q\right\}, \quad (9)$$

assuming an arbitrary discretization operator $\mathcal{D}{:}\mathcal{G}{\to}\mathcal{G}_D$ such as Tustin, forward Euler, zero-order hold etc., and a quantization operator $\mathcal{Q}{:}\mathcal{G}_D{\to}\mathcal{G}_D$, which applies a quantization with step q to each coefficient of $\widetilde{K}(z)$, leading to:

$$\widetilde{K}_q = \left(q\left\lfloor\frac{A_d}{q}\right\rceil, q\left\lfloor\frac{B_d}{q}\right\rceil, q\left\lfloor\frac{C_d}{q}\right\rceil, q\left\lfloor\frac{D_d}{q}\right\rceil\right), \quad (10)$$

described by the matrices (A_d, B_d, C_d, D_d) obtained through $\mathcal{D}\{K, \tau\}$ of (9), and with the rounding operator $\lfloor\cdot\rceil$, applied element-wise to its matrix inputs.

To obtain the discrete-time uncertainty model may be unfeasible if the continuous-time model has been experimentally deduced [21] or it can be deduced with the problem that it is not isomorphic to the continuous-time model, being computed in a different manner. An auxiliary result is that the discretization procedure with the period τ can also applied to $G_n{\mapsto}\widetilde{G}_n$, $U{\mapsto}\widetilde{U}$, $W{\mapsto}\widetilde{W}$, leading to the augmented plant $P{\mapsto}\widetilde{P}$ as in Figure 1–b), maintaining the mappings $\mathcal{T}$, $\mathcal{A}$ from (7), (8), possible according to the following lemma.

Lemma 1: Given the continuous models G_n, U, W, P and mappings $\mathcal{T}(\cdot,\cdot)$, $\mathcal{A}(\cdot,\cdot)$ from (7) and (8), the discrete augmented plant counterpart $\widetilde{P}$ can be computed based on the discretization of its individual components $\widetilde{G}_n$, $\widetilde{U}$, $\widetilde{W}$ through $\mathcal{D}\{\cdot, \tau\}$, $\tau{>}0$. Moreover, the block $\mathbf{\Delta}$ is invariant from the continuous domain to the discrete domain. As such:

$$\widetilde{G} = \mathcal{T}(\mathcal{D}\{G_n, \tau\}, \mathcal{D}\{U, \tau\}),\ \Delta \in \mathbf{\Delta}; \quad (11)$$

$$\widetilde{P} := \mathcal{D}\{P, \tau\} = \mathcal{A}\left(\widetilde{G}, \mathcal{D}\{W, \tau\}\right). \quad (12)$$

Proof: The operators $\mathcal{T}$ and $\mathcal{D}$ are not commutative, so the order of their application is relevant. If the nominal process G_n and the uncertainties U are discretized separately, then the physical significance of the signals presented in Figure 2–a) are also maintained for the case in Figure 2–b), thus resulting an isomorphic representation between G and $\widetilde{G}$. Moreover, considering that $\mathbf{\Delta}$ contains only matrices from $\mathbb{C}^{k\times k}$, the block $\mathbf{\Delta}$ is invariant after applying $\mathcal{T} \circ \mathcal{D}$.

In a similar manner, the operators $\mathcal{A}$ and $\mathcal{D}$ are not commutative, and, in order to keep the physical significance of each signal involved in the augmentation step, the uncertain process $\widetilde{G}$ should be obtained separately from $\widetilde{W}$, the resulting discrete-time uncertain and augmented plant being:

$$\widetilde{P} = \mathcal{A}(\mathcal{T}(\mathcal{D}\{G_n, \tau\}, \mathcal{D}\{U, \tau\}), \mathcal{D}\{W, \tau\}). \quad (13)$$

■

With the previously-defined models $\widetilde{P}$ and $\widetilde{K}_q$, the evaluation of the structured singular value needs to be adapted for the discrete-time case in the following manner:

$$\mu_{\mathbf{\Delta}}(\texttt{LLFT}(\widetilde{P}, \widetilde{K}_q)) = \sup_{\omega\in\Omega_N} \frac{1}{\min\limits_{\Delta\in\mathbf{\Delta}}\{\overline{\sigma}(\Delta), \det(I - \widetilde{M}_\omega\Delta){=}0\}}, \quad (14)$$

with $\widetilde{M}_\omega := \texttt{LLFT}(\widetilde{P}, \widetilde{K}_q)(e^{j\omega\tau})$ and domain $\Omega_N{=}[0, \omega_N)$, where $\omega_N = \pi/\tau$ is the Nyquist frequency for the period τ.

Given that the augmented plant model P encompasses the desired transient and steady-state specifications through the corresponding weighting function W, specifications ensured through the existence of K, a practical approach to obtain the sampling period τ and quantization step q, emphasizing the regulator's implementability on a numeric device, is by solving the following nonlinear optimization problem.

Problem 1: Given a generalized plant model P as in (1) with its corresponding regulator K, with the mechanisms to deduce the discrete-time equivalent $\widetilde{P}$ of (12) and $\widetilde{K}_q$ as in (9) and (10), the *implementability optimization problem* for computing the pair $\xi = (\tau, q) = (\xi_1, \xi_2)$ is defined as:

$$\max_{\xi\in\mathbb{R}_+^2} \xi_1 \cdot \xi_2 \quad \text{s.t.} \quad \mu_{\mathbf{\Delta}}(\texttt{LLFT}(\widetilde{P}, \widetilde{K}_q)) < 1. \quad (15)$$

The expression (15) can be reformulated as a minimization problem without constraints using the interior point method, by employing a logarithmic barrier term [22] as $F_1{:}\mathbb{R}_+^2{\to}\overline{\mathbb{R}}$:

$$F_1(\xi) = -\xi_1{\cdot}\xi_2 - \rho\ln\left(1{-}\mu_\Delta(\texttt{LLFT}(\widetilde{P}, \widetilde{K}_q))\right),\ \rho{>}0, \quad (16)$$

assuming $F_1(\xi){=}\infty$ for ξ where the logarithm is undefined.

The characteristics of the uncertainty weights $\widetilde{U}$ and performance filters $\widetilde{W}$ may be affected by the discretization process. To ensure that, through sampling and discretization, the above functional's solution does not lead to a controller $\widetilde{K}_q$ which fulfills the RS and RP properties for a "different" system, in case of high precision applications, where the hardware constraints of the numerical device are not the main shortcoming, a new optimization problem is proposed.

Problem 2: Given a generalized plant model P as in (1), its corresponding regulator K, with the mechanisms to deduce the discrete-time equivalent $\widetilde{P}$ from (12) and $\widetilde{K}_q$ as in (9), (10), the *fidelity optimization problem* for computing $\xi = (\tau, q)$ with minimum performance loss is defined as:

$$\min_{\xi \in \mathbb{R}_+^2} \mathcal{I}(\xi) \quad \text{s.t.} \quad \mu_{\mathbf{\Delta}}(\texttt{LLFT}(\widetilde{P}, \widetilde{K}_q)) < 1, \tag{17}$$

with the controller similarity integral defined over a frequency range $\Omega \subset [0, \omega_N]$ depending on the variable τ:

$$\mathcal{I}(\xi) = \int_{\Omega} \left| \overline{\sigma}(K) - \overline{\sigma}(\widetilde{K}_q) \right| \left(1 + \left\| \nabla^2 K \right\|\right) d\omega, \tag{18}$$

with the Hessian of the controller's frequency response:

$$\nabla^2 K(j\omega) = \frac{\partial^2}{\partial \omega^2} \left(K(j\omega)\right). \tag{19}$$

Assuming a transfer matrix representation $[K_{ji}]_{\substack{1 \le i \le n_y \\ 1 \le j \le n_u}}$, for an arbitrary SISO component $K_{ji}(s) = \frac{\beta(s)}{\alpha(s)}$, it results that:

$$\nabla^2 K(j\omega) = \left(\frac{\alpha\beta'' - 2\alpha'\beta' - \alpha''\beta}{\alpha^2} + \frac{2\beta\alpha'^2}{\alpha^3} \right) \Bigg|_{j\omega}. \tag{20}$$

The expression (17) can be reformulated as a minimization problem without constraints using the interior point method, by employing a logarithmic barrier term [22] as $F_2 : \mathbb{R}_+^2 \to \overline{\mathbb{R}}$:

$$F_2(\xi) = \mathcal{I}(\xi) - \rho \ln \left(1 - \mu_{\Delta}(\texttt{LLFT}(\widetilde{P}, \widetilde{K}_q))\right), \ \rho > 0, \tag{21}$$

assuming $F_2(\xi) = \infty$ for ξ where the logarithm is undefined.

Remark 1: In the frequency response of $\widetilde{K}_q$, as ω reaches the Nyquist frequency ω_N, a prewarping phenomenon ensues in its magnitude and phase characteristics, which may be minimized by performing the integration up to a smaller upper limit. As such, the set Ω can be replaced in practice by $\Omega \cap (0, \omega_N - \omega_\varepsilon]$, for a prespecified threshold $\omega_\varepsilon > 0$.

The procedure to sample and quantize the regulator in order to maintain RS and RP in discrete-time domain, as a summary of the current section, is presented in Algorithm 1.

Without asserting on the continuity, differentiability and smoothness properties of F_1 and F_2, in particular to the peak structural singular value logarithmic barrier term, consider the relative condition number [23], denoting $F \in \{F_1, F_2\}$:

$$\kappa_F(\xi) = \lim_{\varepsilon \to 0} \sup_{\|\delta\xi\| \le \varepsilon} \frac{\|F(\xi + \delta\xi) - F(\xi)\| / \|\delta\xi\|}{\|F(\xi)\| / \|\xi\|}, \tag{22}$$

along with the two-dimensional ellipse $\mathcal{E} : \mathbb{R}_+^2 \times \mathbb{R}_+^2 \to \mathbb{R}_+^2$:

$$\mathcal{E}(\xi, \delta\xi) = \left\{ x \in \mathbb{R}_+^2 \ \middle| \ \frac{|\xi_1 - x_1|^2}{\delta\xi_1^2} + \frac{|\xi_2 - x_2|^2}{\delta\xi_2^2} < 1 \right\}. \tag{23}$$

Algorithm 1: Optimal selection of sampling rate and quantization step for a continuous-time regulator K

Input: K, G_n, U, W, $\mathcal{T}$, $\mathcal{A}$, $\mathbf{\Delta}$, $F \in \{F_1, F_2\}$, Ω, ρ
Discretization operators $\mathcal{D}_p\{\cdot, \tau\}$, $\mathcal{D}_c\{\cdot, \tau\}$.
{For the plant and controller models}
Solver algorithm $\xi_{k+1} = \Sigma(F, \xi_k)$.
Output: Optimum $\xi^\star = (\tau^\star, q^\star) \in \mathbb{R}_+^2$.

1 Initialize $\xi \leftarrow \xi_0 = (\tau_0, q_0) \in \mathbb{R}_+^2$.
2 **while** *stopping criterion is not satisfied* **do**
3 $\quad \widetilde{G}_n \leftarrow \mathcal{D}_c\{G_n, \xi_1\}$.
4 $\quad \widetilde{U} \leftarrow \mathcal{D}_c\{U, \xi_1\}$; $\widetilde{W} \leftarrow \mathcal{D}_c\{W, \xi_1\}$.
5 $\quad \widetilde{G} \leftarrow \mathcal{T}\left\{\widetilde{G}_n, \widetilde{U}\right\}$; $\widetilde{P} \leftarrow \mathcal{A}\left\{\widetilde{G}, \widetilde{W}\right\}$ {Lemma 1}.
6 $\quad \widetilde{K}_q \leftarrow \mathcal{Q}\{\mathcal{D}\{K, \xi_1\}, \xi_2\}$ {Eq. (9), (10)}.
7 $\quad$ Compute $\mu_{\mathbf{\Delta}}\left(\texttt{LLFT}\left(\widetilde{P}, \widetilde{K}_q\right)\right)$ approximation.
8 $\quad$ Compute $F(\xi)$ {Eq. (16) or (21)}.
9 $\quad$ Update $\xi \leftarrow \Sigma(F, \xi)$.
10 $\quad$ Verify stopping criterion.
11 **end**

To assert the quality and, ultimately, validate the solutions obtained through optimization, a sufficiently high resilience of the condition number with respect to variations around a given nominal value is desired. As such, define for each feasible point $\xi = (\tau, q)$ a *least guaranteed sensitivity bound* $N_F : \mathbb{R}_+^2 \to \mathbb{R}$ for which the relative condition number κ_F remains finite for all points in the encompassing ellipse:

$$N_F(\xi) = \inf_{\varepsilon > 0} \left\{ \kappa_F(x) \in \mathbb{R} \ | \ \forall x \in \mathcal{E}(\xi, \delta\xi), \ \|\delta\xi\| < \varepsilon \right\}, \tag{24}$$

and otherwise, for unfeasible points, defined as zero.

B. Numerical Implementation Aspects

To solve the problems, a global search algorithm [24] was used, based on multiple instances of interior-point nonlinear solvers [25] with forward finite difference derivatives and LDL factorization-based solvers, and instance initializations performed using the scatter search algorithm [26]. Their software counterparts are represented by the `fmincon` and `GlobalSearch` routines from MATLAB®, version R2022a, using several hyperparameter configurations and the built-in `interior-point` algorithm, considering numerical differentiation, with the implicit forward approximation method. The nonconvexity of the optimization problem can lead to a premature stopping of the algorithm into a local minimum point. The solution to practically counteract this phenomenon in most situations is to use the global search to provide multiple starting points for the optimization. The solver Σ implied in Algorithm 1, line 9, uses the previously-mentioned techniques to provide a new pair $\xi = (\tau, q)$ at each new iteration.

There are two main hindrances to guarantee the convergence of Algorithm 1: the NP-hardness of the structured singular value computations, alongside the nonconvexity of the optimization problem, caused by a functional such as F_2

from (21). Regarding the complexity of the algorithm, the following aspects should be considered: the discretization procedures for the plant and regulator, the quantization of the regulator coefficients, the approximation of the SSV and, finally, the inherent steps of the solver Σ.

IV. Numerical Example

The process selected to illustrate the results proposed in Section III is gathered from the benchmark examples of [27], namely a third order industrial process with a non-minimum phase zero and uncertainties, described by:

$$G_n(s) = k_0 \frac{1-\alpha_0 s}{(s+1)^3}, \quad G(s) = k \frac{1-\alpha s}{(s+1)^3}, \qquad (25)$$

with the nominal values α_0=0.1 and $k_0 = 2$, alongside their tolerances $\texttt{tol}_\alpha$=$\pm$10 [%] and $\texttt{tol}_k$=$\pm$5 [%], respectively.

A continuous regulator K is synthesized with the closed-loop shaping methodology [3] using the sensitivity S with weighting function W_S, the complementary sensitivity T with weight W_T, and the control effort $R = KS$ with weight W_R. Their expressions and considered parameters are:

$$W_S(s) = \frac{\frac{1}{M}s + \omega_B}{s + \omega_B A}, \; W_T(s) = \frac{s + \omega_{BT}}{A_T s + \omega_{BT} M_T}, \qquad (26)$$

$W_R(s)$=$1/A_R$, with the parameters ω_B=1.5 $[rad/s]$, M=2, A=10^{-2}, $\omega_{BT} = 15$ $[rad/s]$, $M_T = 2$, $A_T = 2$, $A_R = 10^5$.

The augmented continuous-time plant model, considering the above weighting functions gathered in the block structure W=$\begin{bmatrix} W_S & W_R & W_T \end{bmatrix}^\top$, can be written as:

$$P = \mathcal{A}(G, W) = \begin{bmatrix} W_S & 0 & 0 & 1 \\ -W_S G & W_R & W_T G & -G \end{bmatrix}^\top,$$

and, using the classical D-K iteration μ-synthesis of [15], the resulting state-space regulator K is shown in Equation (27).

Using the zero-order hold discretization method for the process (25), the following analytical expression results:

$$\widetilde{G}_n(z) = \mathcal{D}\{G_n, \tau\} = \frac{k\left(b_1 z^{-1} + b_2 z^{-2} + b_3 z^{-3}\right)}{1 + a_1 z^{-1} + a_2 z^{-2} + a_3 z^{-3}}, \qquad (28)$$

with auxiliary notations γ=$e^{-\tau}$, δ=$\tau\gamma$, $\lambda = \frac{\tau^2}{2}\gamma(1+\alpha)$ and coefficients b_1=$1-\gamma-\lambda-\delta$, b_2=$2\gamma^2+\gamma\left(-2-\lambda-\delta\right)+\lambda+\delta$, b_3=$\gamma\left(-\gamma^2+\gamma+\lambda-\delta\right)$, a_1=-3γ, a_2=$3\gamma^2$, a_3=$-\gamma^3$, $\forall\tau$>0.

The domain of definition for the optimization variable $\xi = (\tau, q)$ is $\mathbf{D} = \left[10^{-7}, 10^{-3}\right] \times \left[10^{-10}, 10^{-4}\right] \subset \mathbb{R}^2_+$, and an identical frequency domain has been used for the similarity integral of (18) for all $\xi \in \mathbf{D}$, namely $\overline{\omega_N} = 95[\%] \cdot \frac{2\pi}{\tau_{\max}} = 5969[rad/s]$, $\Omega = \left[\frac{\overline{\omega_N}}{10^4}, \overline{\omega_N}\right]$, sampled in linear scale. The auxiliary plant terms U, W are discretized using zero-order hold, and the regulator K is discretized using Tustin's method, for a better representation of its frequency response.

Two optimal regulators are obtained, first with the solution $\xi_1^\star = (244.205, 24.4205) \times 10^{-6}$ by solving Problem 1, equivalent to the unconstrained functional (16), along with a solution $\xi_2^\star = \left(4.2739{\times}10^{-6}, 1.02448{\times}10^{-10}\right)$ by solving Problem 2, equivalent to the unconstrained functional (21).

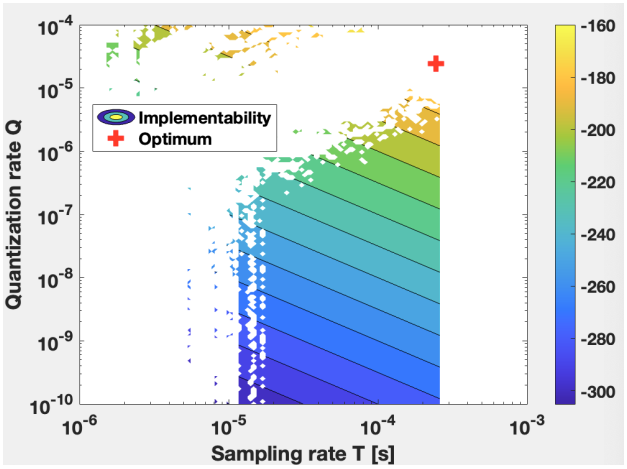

Fig. 3. Feasible region contour plot illustration $[dB]$ of functional (15) for the example process (25) with optimum $\xi_1^\star = (244.205, 24.4205) \times 10^{-6}$.

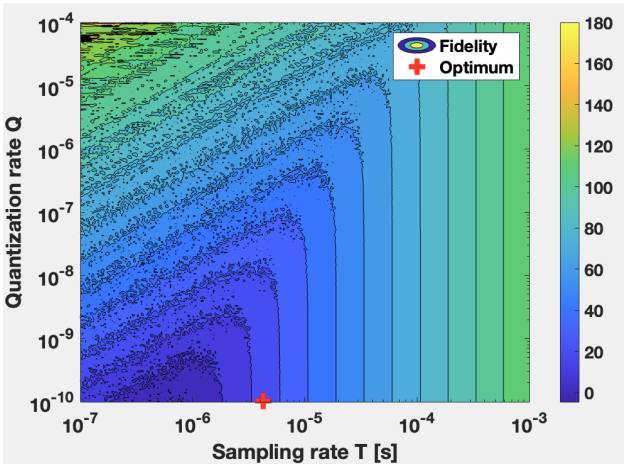

Fig. 4. Functional (17) contour plot for the example process (25) with optimum $\xi_2^\star = \left(4.2739{\times}10^{-6}, 1.02448{\times}10^{-10}\right)$.

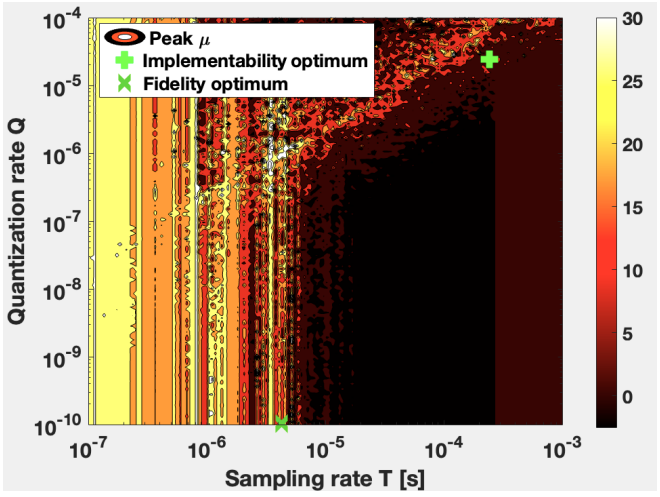

Fig. 5. Peak structured singular value constraint $[dB]$ as function of $\xi \in \mathbb{R}^2_+$. Note that a smaller sampling rate τ, even with a sufficiently small quantization step q does not necessarily lead to a better performing closed-loop system, as the RS and RP criteria may be lost.

$$K(s):\left(\begin{array}{c|c} A_K & B_K \\ \hline C_K & D_K \end{array}\right)=\left(\begin{array}{ccccccc|c} -1.372 & 613.4 & 8.111 & -0.01228 & 7.242 & 0.2304 & -1.163 & 198.4 \\ -613.4 & -1234 & -198.3 & 0.2579 & -233.3 & -7.376 & 37.27 & 5564 \\ -8.111 & -198.3 & -72.1 & 0.145 & -150.4 & -4.655 & 23.65 & 512.1 \\ -0.01299 & -0.4204 & -0.2688 & -0.006131 & -12.27 & 0.5647 & -1.327 & 0.9463 \\ 7.242 & 233.3 & 150.4 & 23.69 & -4357 & -483.1 & 1452 & -524.8 \\ -0.2303 & -7.373 & -4.651 & -0.8474 & 483 & -10.25 & 94.98 & 16.64 \\ 1.161 & 37.27 & 23.64 & 4.143 & -1452 & 95 & -2903 & -84.06 \\ \hline -198.4 & 5564 & 512.1 & -0.5376 & 524.8 & 16.65 & -84.06 & 0 \end{array}\right). \tag{27}$$

The peak approximated SSVs resulted as $\mu_{\mathbf{\Delta}}|_{\xi_1^\star}=0.9781<1$ and $\mu_{\mathbf{\Delta}}|_{\xi_2^\star}=0.9314<1$, with $\mathcal{I}\left(\xi_2^\star\right)=16.06=24.11[dB]$.

The previous results are illustrated in Figures $3, 4, 5$, which show the two-dimensional plots of the cost functions from Problems 1 and 2, along with the SSV feasibility constraint for robustness. The implementability functional plot shows only the feasible areas, with the solution $\xi_1^\star$ found by the global solver, unobservable just by sampling the domain of definition with logarithmically-spaced points.

Remark 2: The authors of [15] warned about the synthesis of discrete-time regulators, which, for small sampling periods, the closed-loop poles tend to gather around $z=1$ and lead to instability or loss of robust performance, with the recommendation of synthesizing the regulator in continuous-time. On the other hand, the experiment presented in this section via the results of Figure 5 showed that this problem remains valid even in case of sampling continuous regulators.

To illustrate the implications on the controller behaviour in open and closed-loop contexts, Figure 6 gathers the open-loop frequency responses for the continuous system KG, the discrete equivalents $\widetilde{K}_q\widetilde{G}$ using the implementability and fidelity solutions, $\xi_1^\star$ and $\xi_2^\star$, along with corresponding closed-loop step response behaviours of said systems, considering a number of 50 Monte Carlo samples from the uncertainty sets, for each of the three cases. Contrary to expectations, while in both discrete cases, the controllers ensure the desired specifications of the sensitivity weights (26), having rise times $t_r\in(0.54,0.77)\,[s]$ and high stability margins, i.e. phase margins $\gamma_k\in(69,79)\,[^\circ]$ and gain margins $m_k\approx 12[dB]$, the implementability solution $\xi_1^\star$, although not as close to the continuous case, guarantees overall better performance, having no overshoot as opposed to $M_p\approx 4.64[\%]$, higher phase margins, and settling times $t_s{\approx}2[s]$, as opposed to $t_s{\approx}4.5[s]$ for the continuous-time case and $\xi_2^\star$.

Remark 3: The fidelity problem solution $\xi_1^\star$, although found to be feasible, leads to numerical instability even when simulated with the standard IEEE 754 floating point with double precision arithmetic. Such difficulties appear in the case of the analytical expression deduced in (28), and also in the case of using the `c2d` function with the `zoh` method from MATLAB© for examples besides the nominal case. The coefficients of the characteristic polynomial of $\widetilde{G}_n$ and corresponding poles are presented in Table I, noting that both computations lead to complex conjugate poles and, additionally, the analytic formula leads to an unstable pole. As such, the simulations for the Monte Carlo experiments implying $\xi_2^\star$ required the use of additional balancing operations.

To further illustrate the numerical properties of solutions $\xi_1^\star$ and $\xi_2^\star$, a numerical approximation of the least guaranteed sensitivity bound (24) was deduced for both cases, using the more demanding function F_2 from (21), for an objective comparison, with 100 Monte Carlo samples per experiment. For $\xi_1^\star$, a relative perturbation $h_1=3.2{\times}10^{-6}$ around $\xi_1^\star$ leads to $N_{F_1}\left(\xi_1^\star\right)\approx 7.8535{\times}10^{-10}$, and $\kappa_{F_2}(x)\in[964.093,7812.503]$, for $x{\in}\mathcal{E}\left(\xi_1^\star,h_1{\cdot}\xi_1^\star\right)$, while a considerably smaller relative perturbation $h_2{=}0.25{\times}10^{-15}$ around $\xi_2^\star$ leads to $N_{F_2}\left(\xi_2^\star\right)\approx 1.0685{\times}10^{-21}$ and $\kappa_{F_2}(x)\in[8.138,84.705]\times 10^{17}$, for $x\in\mathcal{E}\left(\xi_2^\star,h_2{\cdot}\xi_2^\star\right)$. A perturbation of h_1 is tolerable in practice due to stochastic numerical errors, being in the acceptable range for the least significant bit values for τ and q, while the case of $\xi_2^\star$ with a tolerance h_2 yields it unusable. This sensitivity analysis is directly reflected in the structured singular value plots from Figure 7, with relative deviations of 10^{-6} around the computed solutions, and a number of 100 Monte Carlo simulations, showing the ability to consistently maintain robust stability and performance criteria only for the case of $\xi_1^\star$, with $\mu_\Delta\left(\widetilde{P},\widetilde{K}_q\right)<1$, property not maintained around $\xi_2^\star$.

V. Conclusions

The paper proposed a set of mathematical tools to quantify the influence of a constant sampling rate and a fixed-point quantization scheme for the transient response of continuous-time uncertain plant models, by retaining the same modelling framework from the continuous to the discrete domain and maintaining the desired robust stability and performance according to the initially-provided specifications. As emphasized in the provided experiments, the selection of a smaller (τ,q) pair does not necessarily ensure better performance for the closed-loop system. The dichotomic approach of the

TABLE I

High numerical sensitivity of the characteristic polynomial of $\widetilde{G}_n$ for the solution $\xi_2^\star=\left(4.2739{\times}10^{-6},1.02448{\times}10^{-10}\right)$

Case	Parameter	Computed value
1	Ideal $\hat{z}_{1,2,3}$	$\mathbf{0.999995726091887<1}$
2	Analytic a_1	-2.999987178275663
	Analytic a_2	2.999974356606124
	Analytic a_3	-0.999987178330461
2	Analytic $\hat{z}_1$	$\mathbf{1.000005221571111>1}$
	Analytic $\hat{z}_2$	$0.999990978352276+0.000008223234706j$
	Analytic $\hat{z}_3$	$0.999990978352276-0.000008223234706j$
3	`c2d` a_1	-2.999987178275662
	`c2d` a_2	2.999974356606122
	`c2d` a_3	-0.999987178330461
3	`c2d` $\hat{z}_1$	$\mathbf{0.999995723377957<1}$
	`c2d` $\hat{z}_2$	$0.999995727448852+0.000000002350638j$
	`c2d` $\hat{z}_3$	$0.999995727448852-0.000000002350638j$

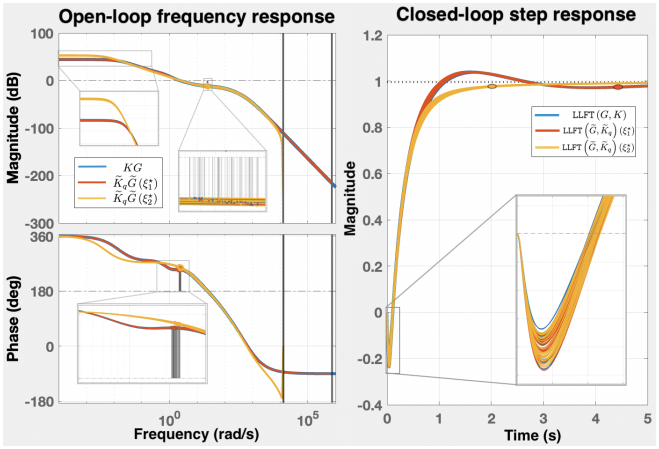

Fig. 6. Open-loop frequency responses using the optimal discretized and quantized regulators $\widetilde{K}_q(z)$ based on $\xi_1^\star$ and $\xi_2^\star$, along with closed-loop step responses, compared to the initial continuous-time case $K(s)$.

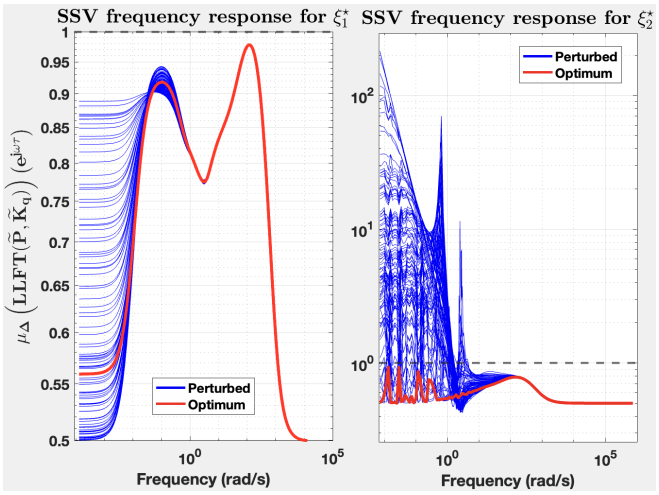

Fig. 7. Structured singular value frequency plots for the two optimal solutions for 10^{-6} relative deviations: $\xi_1^\star$, shown to be insensitive; $\xi_2^\star$, shown to be sensitive by losing desired robust stability and performance.

two proposed optimization problems allows a wide range of means to impose a compromise between fidelity and implementability based on the available hardware of the numerical regulator. A regularization term may be preferred for the fidelity problem to counteract solutions to extreme areas in the domain.

Future work concerns extensions on the modelling framework for discrete-time systems with uncertainties, as the alternative of including parametric uncertainties with direct physical significance leads to transcendental functions, such as discrete poles $e^{\tau/T}$ for arbitrary time constants $T > 0$. On the other hand, a general-purpose extension can be considered based on generic functional F, in which the user may configure it based on the available hardware: τ should be dictated by the operating frequency of the system, whereas q should be determined by the data handling capability, i.e. memory and bandwidth of the system.

References

[1] K. Zhou, J.C. Doyle, K. Glover, *Robust and Optimal Control*, Prentice Hall, Englewood Cliffs, New Jersey, 1995.

[2] D. McFarlane, K. Glover, A loop-shaping design procedure using H/sub infinity / synthesis, *IEEE Transactions on Automatic Control*, vol. 37, no. 6, pp. 759-769, June 1992, doi: 10.1109/9.256330.

[3] S. Skogestad, I. Postlethwaite, *Multivariable Feedback Control: Analysis and Design*; John Wiley & Sons: Hoboken, NJ, USA, 2005.

[4] K.Z. Liu, Y. Yao, Robust Control—Theory and Applications; *John Wiley & Sons*, Singapore, 2016.

[5] P. Apkarian, Nonsmooth μ synthesis. *Int. J. Robust Nonlinear Control*, vol. 21, pp. 1493–1508, 2011, doi:10.1002/rnc.1644.

[6] P. Apkarian, D. Noll. The $\mathcal{H}_\infty$ Control Problem is Solved, *Design and Validation of Aerospace Control Systems*, Aerospace Lab, Alain Appriou, p. 1-11, 2017, doi: 10.12762/2017.AL13-01, ffhal-01653161f.

[7] J.H. Kim, T. Hagiwara, The generalized H_2 controller synthesis problem of sampled-data systems, *Automatica*, Vol. 142, August 2022, 110400, doi:10.1016/j.automatica.2022.110400.

[8] S.F. Tudor, C. Oară, $\mathcal{H}_\infty$ control problem for generalized discrete-time LTI systems, *American Control Conference (ACC)*, pp. 4640-4645, 2015, doi: 10.1109/ACC.2015.7172060.

[9] A. Packard, J. Doyle, G. Balas, Linear Multivariable Robust Control with a μ Perspective. *J. Dyn. Syst. Meas. Ctrl.*, 115, p. 426–438, 1993.

[10] D. Peaucelle, Y. Ebihara, Robust stability analysis of discrete-time systems with parametric and switching uncertainties, *IFAC Proceedings Volumes*, Volume 47, Issue 3, Pages 724-729, 2014, doi:10.3182/20140824-6-ZA-1003.00282.

[11] L. Tan, J. Jiang, *Digital Signal Processing: Fundamentals and Applications*, Third Edition, Academic Press, Elsevier, 2019.

[12] R.H. Middleton, G.C. Goodwin, *Digital Control and Estimation. A Unified Approach*, Prentice Hall, 1990.

[13] M. Şuşcă, V. Mihaly, D. Morar, P. Dobra, Sampling Rate Optimization and Execution Time Analysis for Two-Degrees-of-Freedom Control Systems, *Mathematics*, 10, 3449, 2022, doi:10.3390/math10193449.

[14] M. Susca, V. Mihaly, P. Dobra, Sampling rate selection for multi-loop cascade control systems in an optimal manner, *IET Control Theory & Applications*, Wiley, pp. 1–15, 2023, doi:10.1049/cth2.12444.

[15] G. Balas, R. Chiang, A. Packard, M. Safonov, *Robust Control Toolbox^{TM}, Reference*, Version 6.11.2 (R2022b), September, 2022.

[16] M. Şuşcă, V. Mihaly, P. Dobra, Fixed-Point Uniform Quantization Analysis for Numerical Controllers, *2022 IEEE Conference on Decision and Control* (CDC), Cancún, Mexico, 2022, doi:10.1109/CDC51059.2022.9993223.

[17] X. Xu, N. Ozay, V. Gupta, Passivity-based analysis of sampled and quantized control implementations, *Automatica*, Vol. 119, Sept., 2020.

[18] A. Bicchi, A. Marigo and B. Piccoli, On the reachability of quantized control systems, *IEEE Transactions on Automatic Control*, vol. 47, no. 4, pp. 546-563, April 2002, doi: 10.1109/9.995034.

[19] G. Kreisselmeier, On sampling without loss of observability/controllability, *IEEE Transactions on Automatic Control*, vol. 44, no. 5, pp. 1021-1025, May 1999, doi: 10.1109/9.763221.

[20] W. Liu, J. Sun, G. Wang, F. Bullo, J. Chen, Resilient Control Under Quantization and Denial-of-Service: Codesigning a Deadbeat Controller and Transmission Protocol, *IEEE Transactions on Automatic Control*, vol. 67, no. 8, pp. 3879-3891, Aug. 2022, doi: 10.1109/TAC.2021.3107145.

[21] H. Hindi, C.-Y. Seong, S. Boyd, Computing optimal uncertainty models from frequency domain data, *Proceedings of the 41st IEEE Conference on Decision and Control*, pp. 2898-2905 vol. 3, 2002.

[22] Y. Nesterov, *Lectures on Convex Optimization*, Ed. 2, Springer, 2010.

[23] N.J. Higham, *Accuracy and Stability of Numerical Algorithms*, Second Edition, SIAM Philadelphia, ISBN 0-89871-521-0, 2002.

[24] Z. Ugray, L. Lasdon, J. Plummer, F. Glover, J. Kelly, R. Martí, Scatter Search and Local NLP Solvers: A Multistart Framework for Global Optimization, *INFORMS Journal on Computing*, 19(3):328-340, 2007, doi:10.1287/ijoc.1060.0175.

[25] R. Byrd, J. Gilbert, J. Nocedal, A trust region method based on interior point techniques for nonlinear programming, *Math. Program.*, 89, 149–185, 2000, doi:10.1007/PL00011391.

[26] F. Glover, A template for scatter search and path relinking, in *Hao, JK., Lutton, E., Ronald, E., Schoenauer, M., Snyers, D. (eds) Artificial Evolution. AE 1997. Lecture Notes in Computer Science*, vol. 1363. Springer, Berlin, Heidelberg, 1998, doi:10.1007/BFb0026589.

[27] K.J. Åström, T. Hägglund, Benchmark Systems for PID Control, *IFAC Proceedings*, vol. 33, issue 4, pp. 165–166, April 2000.